Frontiers in Bioscience Landmark

Front. Biosci. (Landmark Ed) **2022**; 27(11): 316
https://doi.org/10.31083/j.fbl2711316

Original Research

Comparison of the Pathogenicity of SARS-CoV-2 Delta and Omicron Variants by Analyzing the Expression Patterns of Immune Response Genes in K18-hACE2 Transgenic Mice

Kuruppu Arachchillage Praboda Priyangi Kuruppuarachchi[1,2,†], Yunyueng Jang[1,2,†], Sang Heui Seo[1,2,*]

[1]Laboratory of Influenza Research, College of Veterinary Medicine, Chungnam National University, 34134 Daejeon, Republic of Korea
[2]Institute of Influenza Virus, Chungnam National University, 34134 Daejeon, Republic of Korea
*Correspondence: seos@cnu.ac.kr (Sang Heui Seo)
[†]These authors contributed equally.

Academic Editor: Vijay Kumar
Submitted: 3 September 2022 Revised: 8 November 2022 Accepted: 9 November 2022 Published: 30 November 2022

Abstract

Background: The recently emerged variants of the severe acute respiratory coronavirus 2 (SARS-CoV-2) pose a threat to public health. Understanding the pathogenicity of these variants is a salient factor in the development of effective SARS-CoV-2 therapeutics. This study aimed to compare the expression patterns of genes involved in immune responses in K18-hACE2 mice infected with the wild-type, Delta, and Omicron SARS-CoV-2 variants. **Methods**: K18-hACE2 mice were intranasally infected with either wild-type (B.1), Delta (B.1.617.2), or Omicron (B.1.1.529) variants. On day 6 post-infection, lung, brain, and kidney tissues were collected from each variant-infected group. The mRNA expression levels of 39 immune response genes in all three groups were compared by RT-qPCR. Viral titers were measured using the median tissue culture infectious dose ($TCID_{50}$) assay and expressed as Log10 $TCID_{50}$/0.1 g. The statistical significance of the differences in gene expression was determined by one-way analysis of variance (ANOVA) (alpha = 0.05). **Results**: The expression of toll-like receptors (TLRs) was upregulated in the lung and brain tissues of the wild-type- and Delta-infected groups but not in those of the Omicron-infected group. The highest expression of cytokines, including interleukin (*IL*)-*1*α, *IL-1*β, *IL-17*α, interferon, and tumor necrosis factors, was observed in the lungs of mice infected with the wild-type variant. Additionally, *CCL4*, *CCL11*, *CXCL9*, and *CXCL10* were upregulated (>3-fold) in wild-type-infected mice, with markedly higher expressions in the brain than in the lungs. Most of the apoptotic factors were mainly expressed in the brain tissues of Omicron-infected mice (*caspase 8*, *caspase 9*, *p53*, *Bax*, *Bak*, *BCL-2*, and *Bcl-XL*), whereas neither the lung nor kidney showed more than 3-fold upregulation of these apoptotic factors. **Conclusions**: Collectively, our findings revealed that the wild-type SARS-CoV-2 variant exhibited the highest pathogenicity, followed by the Delta variant, then the Omicron variant.

Keywords: apoptosis; cytokines; Delta; Omicron; SARS-CoV-2; viral pathogenicity

1. Introduction

The outbreak of the coronavirus-associated acute respiratory disease (COVID-19), caused by the severe acute respiratory syndrome coronavirus 2 (SARS-CoV-2), first emerged in China (Hubei Province) in December 2019 [1]. SARS-CoV-2 has a positive single-stranded, non-segmented RNA genome, and its virion comprises four major structural proteins: the nucleocapsid (N), transmembrane (M), envelope (E), and spike (S) proteins [2]. The receptor-binding domain (RBD) of the S proteins interacts with the host receptor, angiotensin-converting enzyme 2 (ACE2), invading epithelial cells in the respiratory and gastrointestinal tracts [3].

SARS-CoV-2 continuously evolves via genetic mutations, mainly in the spike genes, and circulates in the human population, causing viral adaptation to human cells [4]. In March 2021, the World Health Organization (WHO) declared nomenclature for global SARS-CoV-2 variants of concern (VOC), such as Delta and Omicron, and variants of interest (VOI), such as Alpha, Beta, and Gamma [5]. The SARS-CoV-2 Delta (B.1.617.2) variant is 40–60% more transmissible than the Alpha variant (B.1.1.7), increasing the risk of hospitalization [6]. Eight mutations have been identified in the S protein of the Delta variant (T19R, G142D, del157/158, L452R, T478K, D614G, P681R, and D960N), two of which (L452R and T478K) are in the RBD of the S protein [7]. Following the emergence of the Delta variant, a distinct variant emerged and was identified as Omicron (B.1.1.529) by the WHO on November 24, 2021 [8]. An epidemiological study has reported a 48% increased risk of transmission when infected with the Omicron variant than with the Delta variant, owing to the markedly high binding affinity of the Omicron variant with human ACE2 [1,6]. However, the Omicron variant is associated with lower disease severity than the Delta variant, with a case fatality ratio of 1.9% versus 3.4% for Delta [9].

The immune system detects SARS-CoV-2 infection by recognizing pathogen-associated molecular patterns (PAMPs), triggering the production of several inflammatory cytokines and chemokines, including interleukin *IL-1*β, *IL-2*, *IL-6*, *IL-7*, *IL-8*, *IL-9*, *IL-10*, *IL-17*, *IL-18*, *IL-22*, *IL-33*, granulocyte-colony-stimulating factor (*G-CSF*), granulocyte-macrophage colony-stimulating factor (*GM-CSF*), interferon (*IFN*)-γ, tumor necrosis factor (*TNF*)-α, chemokine ligand (*CXCL*)*10*, monocyte chemoattractant protein 1 (*MCP-1*) *A*, *CX3CL1*, and macrophage inflammatory protein-1beta (MIP-1β)/(*CCL4*) [10]. This cytokine storm results in an inflammatory response that is associated with acute respiratory distress syndrome (ARDS), a SARS-CoV-2-associated complication [11].

The pathogenicity and virulence of the SARS-CoV-2 ancestral strain and other VOCs, including Delta and Omicron, have been mainly investigated using clinical samples from hospitalized patients and *in silico* studies. However, *in vivo* studies on the pathogenicity of VOCs have been limited. Transgenic mice with human angiotensin I-converting enzyme 2 (hACE2) receptor and promoter cytokeratin 18 (K18; K18-hACE2) are well-established animal models that can reproduce human SARS-CoV-2 infection [12–15]. Mouse models mimic the gene expression patterns of human inflammatory genes [16]; therefore, they have been used to evaluate the pathogenicity of human SARS-CoV-2 and the efficacy of prophylactics and therapeutics against infections [17–19].

SARS-CoV-2 associated complications have been reported to be triggered by the expression of different patterns of immune response genes. Therefore, a comprehensive understanding of these expression patterns is paramount for developing effective therapeutics for SARS-CoV-2 infections and terminating the pandemic. However, there is a lack of studies evaluating the pathogenicity of Delta and Omicron variants by comparing the gene expressions of immune-related genes. This study aimed to evaluate and compare the differences in the mRNA expression patterns of cytokines, chemokines, and apoptotic factors in K18-hACE2 transgenic mice infected with the ancestral strain, Delta, and Omicron variants.

2. Materials and Methods

2.1 Animals

Female K18-hACE2 transgenic mice [B6. Cg - Tg (K18-ACE2)2Prlmn/J; 6–7 weeks old] were acquired from the Jackson Laboratory (Bar Harbor, ME, USA). The mice were regularly fed a standard chow diet and water.

2.2 Virus and Cells

SARS-CoV-2 viruses were provided by the Korea Center for Disease Control (KCDC): wild-type [SARS-CoV-2/Korea/KCDC03/2020(B.1)], Delta variant [hCoV-19/Korea/KDCA119861/2021(B.1.617.2)], and Omicron variant [hCoV-19/Korea/KCDC447321/2021(B.1.1.529)]. All viruses were propagated in Vero-E6 cells obtained from American Type Culture Collection (VERO C1008, Manassas, VA, USA). Vero E6 cell cultures were maintained in minimal essential medium (MEM) supplemented with 10% fetal bovine serum (FBS) and 1$\times$ antibiotic-antimycotic solution (Sigma-Aldrich, St. Louis, MO, USA).

All experiments with SARS-CoV-2 were performed in a biosafety level -3 (BSL-3) facility certified by the Korean government.

2.3 Infection of hACE2 Transgenic Mice with SARS-CoV-2 Variants

K18-hACE2 transgenic mice (n = 10 per group) were intranasally infected with 50 μL of 1 $\times$ 10^4 PFU/mL wild-type, Delta, or Omicron variants after being anesthetized using isoflurane USP (Troikaa Pharmaceuticals Ltd., Gujarat, India). Infected mice were monitored for up to 14 days post-infection (d.p.i). K18-hACE2 transgenic mice (n = 5) were inoculated with 50 μL phosphate buffered saline (PBS) as control.

2.4 Measurement of Body Weight and Survival Rates

The survival of the mice infected with the three SARS-CoV-2 variants was monitored for 14 d.p.i. The change in body weight of the surviving mice after infection was measured at a two-day interval for 14 d.p.i. or until death. Similarly, the body weight of PBS mock K18-hACE2 transgenic mice (n = 5) was measured as a control.

2.5 Measurement of Viral Titers

Lung, brain, and kidney tissues were isolated from wild-type-, Delta-, and Omicron-infected mice on day 6 p.i. Each tissue (0.1 g) was homogenized with 1 mL of PBS (pH 7.40). The homogenized solutions were filtered using 0.2 μm syringe filters and centrifuged to obtain the supernatant. The supernatants were serially diluted in MEM with 1.5% bovine serum albumin (BSA) to obtain a 10-fold dilution.

Vero cells were cultured in 96-well cell culture plates in MEM supplemented with 10% FBS and 1$\times$ antibiotic-antimycotic solution and incubated at 37 °C in a humidified incubator. After reaching 80% confluence, Vero cells were washed with warm PBS (pH 7.40). Then, 100 μL of the diluted supernatant from each tissue sample was added to the Vero cell culture and incubated at 37 °C for 4 days in a humidified incubator.

After fixation, cells were permeabilized with 80% cold acetone (Samchun Pure Chemical Co., Seoul, Republic of Korea). SARS-CoV-2 nucleocapsid rabbit polyclonal antibody (Thermo Fisher Scientific, Waltham, MA, USA) was added to the cells, followed by incubation with fluorescently labeled goat anti-rabbit antibody (Thermo Fisher Scientific, Waltham, MA, USA). Endpoint titers were evaluated using the Muench and Reed method [20].

2.6 Quantification of Inflammatory Cytokines, TLRs, and Apoptotic Factors by Real-Time Quantitative PCR

2.6.1 RNA Extraction

Total RNA was extracted from infected mice using the TRIzol RNA extraction kit. Lung, brain, and kidney tissues were obtained from wild-type-, Delta-, and Omicron-infected mice (n = 3 per group) at 6 d.p.i. Each tissue sample (0.1 g) was treated with 1 mL TRIzol reagent (Invitrogen, Carlsbad, CA, USA) and incubated at room temperature for 5 min. Chloroform (200 μL; Sigma-Aldrich, St. Louis, MO, USA) was added to the TRIzol solution and vortexed for 15 s, followed by centrifugation at 12,000 rpm and 4 °C for 10 min. The aqueous phase containing RNA was transferred to a new 1.5 mL microcentrifuge tube. Isopropanol (500 μL; Samchun Pure Chemical Co., Seoul, Republic of Korea) was added to each tube and centrifuged at 10,000 rpm at 4 °C for 10 min. The resulting RNA pellet was washed with 100 μL of 75% ethanol and centrifuged at 10,000 rpm at 4 °C for 5 min. Finally, the RNA was resuspended in 50 μL nuclease-free water.

2.6.2 cDNA Synthesis

cDNA was synthesized using 2.5 μg of RNA and 1 μL of 0.5 μM of oligo dT primer (Promega, Madison, WI, USA) by an initial incubation at 70 °C for 5 min and cooling to 4 °C for 5 min. The reaction mixture contained 4 μL of 5 $\times$ reverse transcriptase enzyme buffer, 4 μL of 25 mM $MgCl_2$, 1 μL of 10 mM nucleotide mixture, 1 μL of reverse transcriptase enzyme, and 0.5 μL of RNase inhibitor at 4 °C and was further incubated at 25 °C for 5 min, 42 °C for 60 min, and 70 °C for 15 min.

2.6.3 Analysis of Gene Expression Levels

RT-qPCR was performed to analyze the expression levels of genes encoding cytokines, chemokines, TLRs, and apoptotic factors in the lung, brain, and kidney of SARS-CoV-2 variant-infected mice. The RT-qPCR reaction was set up for a total volume of 20 μL containing 10 μL of TOPreal^{TM} qPCR 2 $\times$ Premix (SYBR Green with low ROX) (Enzynomics Inc., Daejeon, South Korea), TLR, cytokines, chemokines, and apoptotic factors-specific primers (**Supplementary Table 1**); 1 μL of each forward and reverse primer (10 pmol) and 2 μL of 350 ng/μL cDNA. Duplicates of each reaction were performed with 45 PCR cycles (denaturation at 95 °C for 10 s, annealing at 60 °C for 15 s, and elongation at 72 °C for 15 s) in a Rotor-Gene 6000 apparatus (Corbett Life Science, Mortlake, Australia). Gene expression levels in tissues were normalized using the mouse *beta-actin* gene. Relative fold change in gene expression was calculated using the $2^{-\Delta\Delta Ct}$ method. Gene expression levels in the lungs, brain, and kidneys of uninfected mice (n = 1) were used as controls.

2.7 Lung Pathology Analysis

To determine tissue histopathology, the lung tissues of mice infected with SARS-CoV-2 variants (n = 3 per group) were collected at 6 d.p.i., fixed in 10% phosphate-buffered formalin (Triangle Biomedical Sciences, General Data Healthcare, Cincinnati, OH, USA) for 6 h, washed with running tap water, and embedded in paraffin. Tissue sections (5 μm) were prepared and stained with Harris hematoxylin for 1 min and 30 s and 1% Eosin Y solution for 1 min and 30 s. The stained tissues were mounted on Canada balsam and observed for pneumonia-related signs using an Olympus DP70 microscope (Olympus Corporation, Tokyo, Japan).

2.8 Statistical Analysis

Statistical significance was determined using the unpaired two-tailed *t*-test method, and one-way analysis of variance (ANOVA) alpha = 0.05. Data were analyzed using the GraphPad Prism software (version 8.0.1) (Dotmatics, San Diego, CA, USA).

3. Results

3.1 Changes in the Survival Rate and Body Weight of Mice Infected with SARS-CoV-2

To compare the differences in survival rates after infections with the SARS-CoV-2 variants, we infected K18-hACE2 mice with wild-type, Delta, or Omicron variants (n = 10 per group) and observed mortality and body weight for 14 days. All mice that received the wild-type virus died within 7 days. Delta-infected mice showed 100% survival until 7 d.p.i, then died within two days. However, all mice infected with the Omicron variant and mock PBS exhibited a 100% survival rate until 14 d.p.i. (Fig. 1A).

Wild-type and Delta-infected mice started to lose body weight after 4 d.p.i. and showed 83% and 71% initial mean body weight at 6 d.p.i., respectively. Interestingly, the body weight of Omicron-infected mice increased at 6 d.p.i. and reached 110.5% of the initial mean body weight at 14 d.p.i., whereas mock mice reached 125% of the mean body weight (Fig. 1B). These results indicate that the Omicron group exhibited body weight gain, similar to the mock group, whereas the wild-type and Delta groups showed body weight reduction. However, these differences were not statistically significant.

3.2 Viral Loads in Infected Lung Tissues

The viral titers in each tissue of the infected mice were measured using the Log10 median tissue culture infectious dose ($TCID_{50}$) assay at 6 d.p.i. Wild-type- and Delta-infected mice showed similar viral titers in the nasal turbinate, brain, and kidney tissues. In the brain, the viral titers in wild-type- and Delta-infected mice (8.5 $TCID_{50}$/0.1 g and 9.5 Log10 $TCID_{50}$/0.1 g) were significantly higher than those in Omicron-infected mice (4.5 $TCID_{50}$/0.1 g). The viral titers in the lung tissues were the

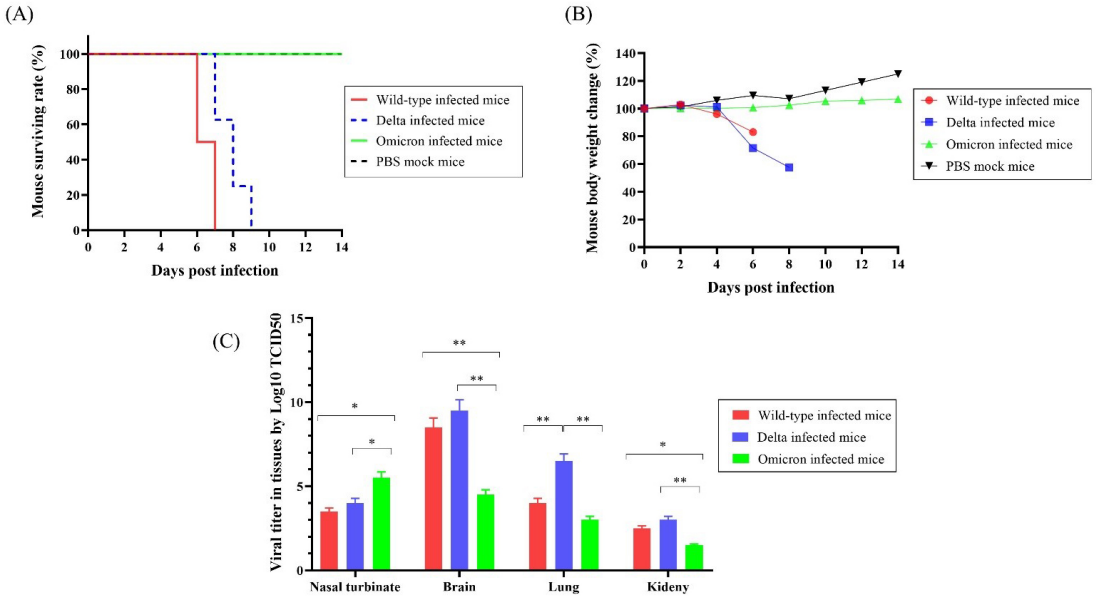

Fig. 1. The surviving rate, body weight changes, and viral titers of K18-hACE2 transgenic mice infected with the SARS-CoV-2 variants (n = 10 per group). (A) Survival rate of mice infected with wild-type, Delta, and Omicron SARS-CoV-2 and uninfected mice. (B) Body weight changes after infection with wild-type, Delta, Omicron, and PBS. (C) Viral titers in tissues of mice infected with wild-type, Delta, or Omicron determine by Log10 $TCID_{50}$/0.1 g. * $p < 0.05$, ** $p < 0.01$.

highest in the Delta group (6.5 $TCID_{50}$/0.1 g), followed by the wild-type group (4 $TCID_{50}$/0.1 g), and the Omicron group (3 $TCID_{50}$/0.1 g). The viral titers in the brain, lung, and kidney of Omicron-infected mice were lower than those of the other variant-infected mice. The viral titers in the nasal turbinate were the highest in the Omicron group (5.5 $TCID_{50}$/0.1 g), followed by the Delta group (4 $TCID_{50}$/0.1g), then the wild-type group (3.5 $TCID_{50}$/0.1 g) (Fig. 1C).

3.3 Analysis of Gene Expression Levels of Immune Response Genes During SARS-CoV-2 Infections

To evaluate the pathogenicity of the wild-type, Delta, and Omicron SARS-CoV-2 variants at the molecular level, we analyzed the expression levels of 39 immune response genes in the lung, brain, and kidney tissues of mice collected at 6 d.p.i. by RT-qPCR. The selected 39 immune response genes belong to various functional categories, including *TLR*s, cytokines, chemokines, and apoptotic factors. Relative gene expression levels were determined by relative fold change based on the gene expression levels of the PBS mock-treated group. The differential expression of each gene in different tissues of the wild-type, Delta, and Omicron groups is illustrated and summarized in a heatmap (Figs. 2,3,4,5,6 and **Supplementary Figs. 1,2**).

3.3.1 TLR expression

To identify innate immune activation following SARS-CoV-2 infection, we evaluated *TLR* gene expression in the lung, brain, and kidney of wild-type-, Delta-, and Omicron-infected mice. *TLR1*, *TLR2*, and *TLR7* were upregulated (>3-fold) in the lung tissues of both wild-type- and Delta-infected mice (Fig. 2A). TLR8 was upregulated by 3.59-fold only in the lung tissues of mice infected with the wild-type variant compared to control mice (Figs. 2A,3A). However, *TLR1* and *TLR7* were both significantly upregulated ($p < 0.0001$) in the lungs of wild-type- and Delta-infected mice (Fig. 3A). Similar to the lungs, the kidneys of wild-type- and Delta-infected mice showed upregulation of *TLR2* (4.74-fold and 4.09-fold, respectively; Fig. 3C). *TLR2* expression in the brain of the wild-type group was markedly higher (31.15-fold) than that in the brain of the control group (Fig. 3B). Moreover, *TLR8* and *TLR9* were upregulated in the brains and kidneys of the wild-type and Delta groups, respectively (>3-fold; Fig. 2A). *TLR7* was upregulated in the brains of wild-type-infected mice (6.95-fold, $p < 0.001$) and the kidneys of Omicron- and Delta-infected mice (3.08-fold and 3.84-fold, respectively) compared to the control group (Fig. 3B,C). Furthermore, *TLR5*, *TLR8*, and *TLR1* were considerably downregulated (<3-fold) in the brains and kidneys of Delta-infected and wild-type-infected mice, respectively (Figs. 2B,3B,C).

Overall, these results indicate that infections with the wild-type and Delta SARS-CoV-2 resulted in increased *TLR* expression in the lung and brain tissues, whereas infection with the Omicron variant did not.

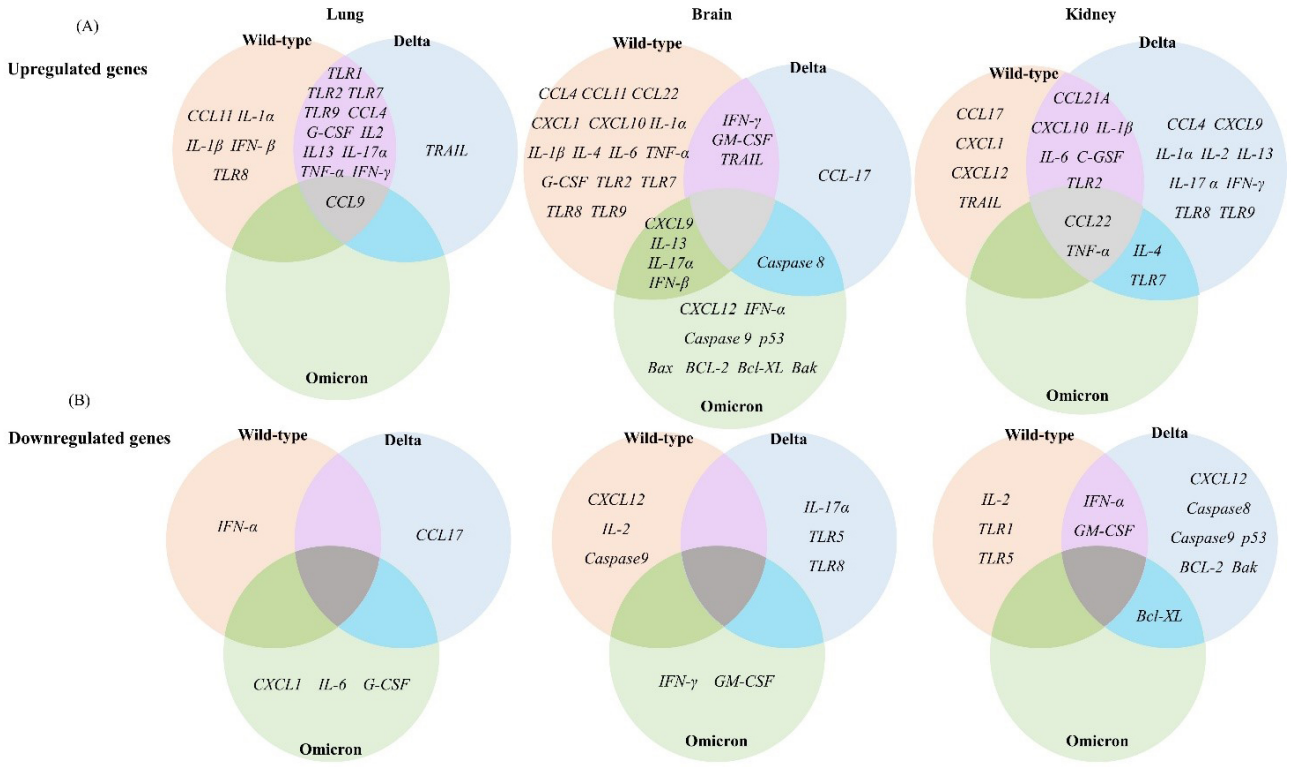

Fig. 2. Differential expression of immune response genes in K18-hACE2 transgenic mice after infections with the SARS-CoV-2 variants. (A) Upregulated mRNA expression of genes related to the immune response in the lung, brain, and kidney tissues of wild-type-, Delta-, or Omicron-infected mice. (B) Downregulated mRNA expression of genes related to the immune response in the lung, brain, and kidney after infection with wild-type, Delta, or Omicron (>3-fold change = upregulation and <3-fold change = downregulation).

3.3.2 Cytokine Expression

IL-1α and *IL-1β* were highly expressed in the lung and brain tissues of mice infected with the wild-type. In the kidney, *IL-1α* was upregulated only after infection with the Delta variant, whereas *IL-1β* was upregulated after infections with the Delta variant and wild-type. Upregulation of *IL-2* was only observed in the lungs of the wild-type- and Delta-infected groups and kidneys of the Delta-infected group. However, *IL-2* was downregulated in the kidneys (0.29-fold) and brain (0.16-fold) of wild-type-infected mice. *IL-13* was overexpressed (947.68-fold) in the kidneys of Delta-infected mice, lung tissues of wild-type- or Delta-infected mice, and brains of wild-type- or Omicron-infected mice (Figs. 2A,4A–C).

IL-4 and *IL-6* expression levels were upregulated by 5.43 and 51.65, respectively, in the brain tissues following infection with the wild-type, and the increase in *IL-6* expression was statistically significant ($p < 0.001$). The kidney tissues of both wild-type- and Delta-infected mice showed upregulated *IL-6* expression levels by 3.65-fold and 14.38-fold, respectively. Surprisingly, *IL-6* was significantly downregulated (0.05-fold, <0.01) in the lung tissues of Omicron-infected mice, whereas it was expressed at basal levels in the lungs of wild-type- and Delta-infected mice (Figs. 2B,4A–C).

IL-17A was moderately upregulated in lung tissues after infection with the wild-type or the Delta variant by 12.0-fold and 8.91-fold, respectively. The brain tissues of wild-type- and Omicron-infected mice exhibited increased *IL-17A* expression levels by 21.27-fold and 7.40-fold, respectively, whereas those of Delta-infected mice showed drastic *IL-17A* downregulation compared to the control. Interestingly, *IL-17A* expression levels were markedly increased in the kidney after infections with wild-type, or Delta and Omicron variants compared to the control (Fig. 4A–C).

In addition, we evaluated the expression levels of *IFN* and *TNF* in the lungs, brain, and kidneys of the mice infected with the three variants. *IFN-α*, *IFN-β*, and *IFN-γ* were differentially expressed in the lungs, brain, and kidneys of all three groups. Significantly increased *IFN-γ* expression levels were observed in the lungs and brains (>3-fold increase) of wild-type- and Delta-infected mice and the kidneys of Delta-infected mice. However, *IFN-γ* expression was downregulated (>3-fold) in the brain tissues of Omicron-infected mice. *IFN-α* was upregulated in the brain tissues of Omicron-infected mice and downregulated (<3-fold) in both the lungs and kidneys of wild-type-infected mice and in the kidneys of Delta-infected mice. TNF-α was upregulated by more than 3-fold in all tissues of wild-type-infected mice and kidneys of mice infected with

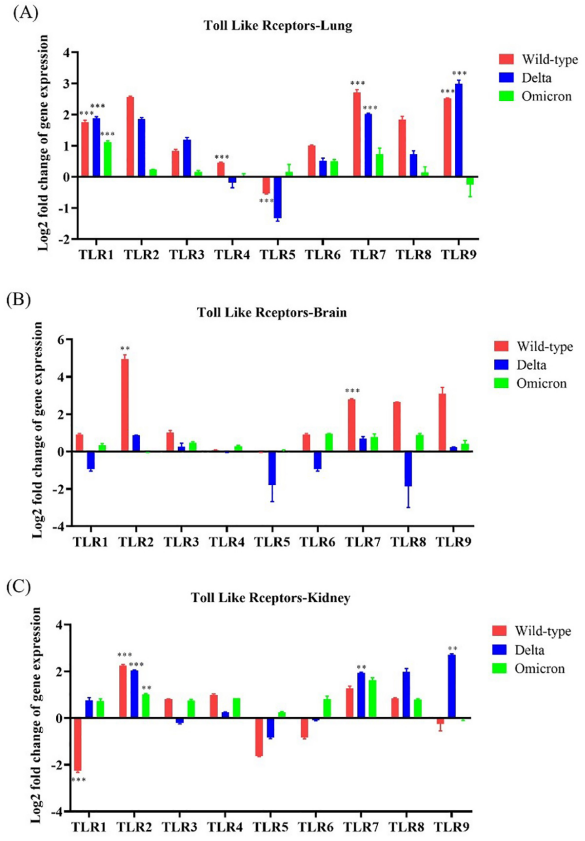

Fig. 3. Toll-like receptor (*TLR*) gene expression in the lung, brain, and kidneys of K18-hACE2 transgenic mice infected with SARS-CoV-2 variants. The mRNA expression of each gene was normalized to that of mouse β-actin mRNA, and the fold changes were calculated using the $2^{-\Delta\Delta CT}$ method. Statistically significant differences in gene expression levels between each group compared to PBS mock-infected mice (n = 3) were analyzed using an unpaired two-tailed *t*-test. * $p < 0.05$, ** $p < 0.01$, *** $p < 0.001$, **** $p < 0.0001$. (A) *TLR* gene expression in the lung tissues of wild-type-, Delta-, and Omicron-infected mice. (B) *TLR* gene expression in the brain tissues of wild-type, Delta-, and Omicron-infected mice. (C) *TLR* gene expression in kidney tissues of wild-type-, Delta-, and Omicron-infected mice.

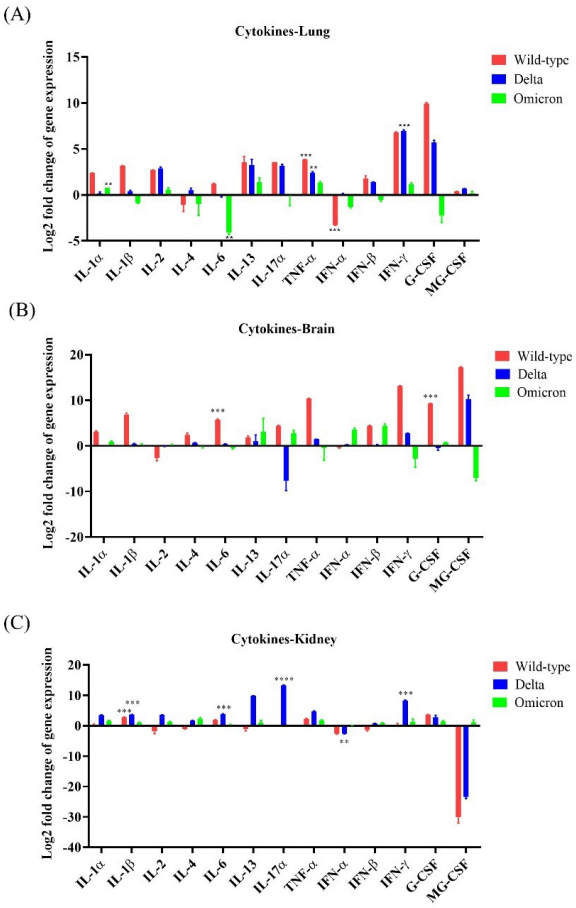

Fig. 4. Cytokine expression in K18-hACE2 mice after infections with SARS-CoV-2 variants. The expression levels of 13 cytokine genes (seven interleukins, *TNF-α*, interferon type I and II, *G-CSF*, and *MG-CSF*) were evaluated after infections with wild-type, Delta variant, or Omicron variant. (A) mRNA expression of cytokine-related genes in the lungs after inoculation with wild-type, Delta, or Omicron. (B) mRNA expression of cytokine-related genes in the brain after inoculation with wild-type, Delta, or Omicron. (C) mRNA expression of cytokine-related genes in the kidney after inoculation with wild-type, Delta, or Omicron. * $p < 0.05$, ** $p < 0.01$, *** $p < 0.001$, **** $p < 0.0001$.

Delta or Omicron. In addition, *G-CSF* was upregulated in the lungs of wild-type- and Delta-infected mice and the brains of wild-type-infected mice (Figs. 2A,B,4A–C).

Overall, these results indicate that cytokine production was the highest in the lungs of mice infected with wild-type compared to that in different tissues of the other groups.

3.3.3 Chemokine Expression

The lungs, brain, and kidneys of wild-type-infected mice showed the highest chemokine expression compared to the other infected groups. Overall, *CCL4*, *CCL11*, *CXCL9*, and *CXCL10* were upregulated (>3-fold) in both the lungs and brains of wild-type-infected mice and were markedly higher in the brain than in the lung. *CCL4* expression was significantly upregulated in the lung and brain by 29.54-fold and 648.91-fold, respectively, of wild-type-infected mice compared to that in control mice. The expression levels of *CXCL1* and *CXCL12* were reduced in the lungs and brain, respectively, in response to infection with the Delta variant. However, when mice were challenged with the Omicron variant, *CXCL9* was upregulated by 5.08-fold and 5.89-fold in the lung and brain, respectively. *CXCL12* and *CCL22* were only upregulated in the brain (4.49-fold) and kidney (3.64-fold) of Omicron-infected mice, respectively. *CCL17* was significantly upregulated (3.83-fold) in the brain of Delta-infected mice

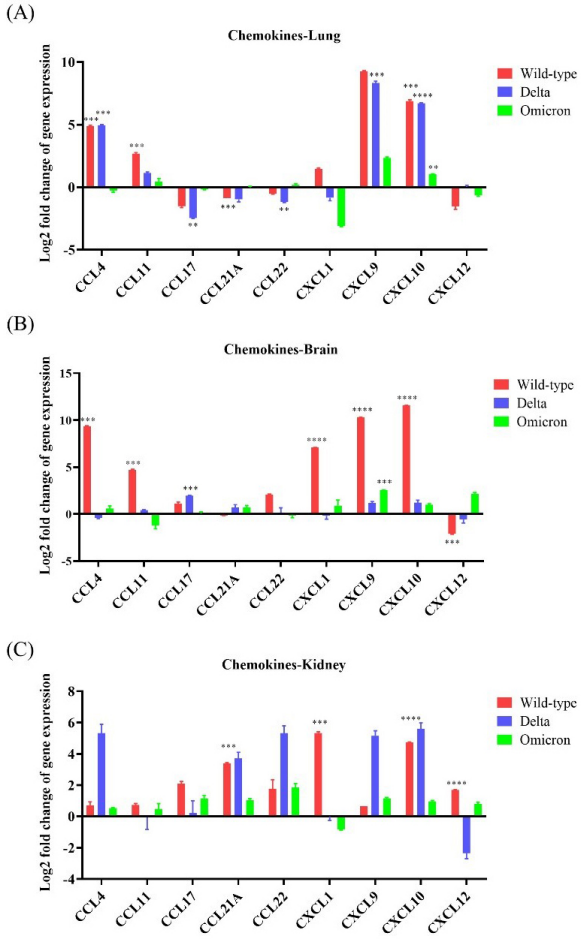

Fig. 5. Chemokine expression in K18-hACE2 mice infected with SARS-CoV-2. The mRNA expression levels of nine chemokine genes (*CCL4*, *CCL11*, *CCL17*, *CCL21A*, *CCL22*, *CXCL1*, *CXCL9*, *CXCL10*, and *CXCL12*) were evaluated after infection with wild-type, Delta variant, or Omicron variant. (A) mRNA expression of the chemokine genes in the lung after inoculation with wild-type, Delta, or Omicron. (B) mRNA expression of the chemokine genes in the brain after inoculation with wild-type, Delta, or Omicron. (C) mRNA expression of the chemokine genes in the kidney after inoculation with wild-type, Delta, or Omicron. * $p < 0.05$, ** $p < 0.01$, *** $p < 0.001$, **** $p < 0.0001$.

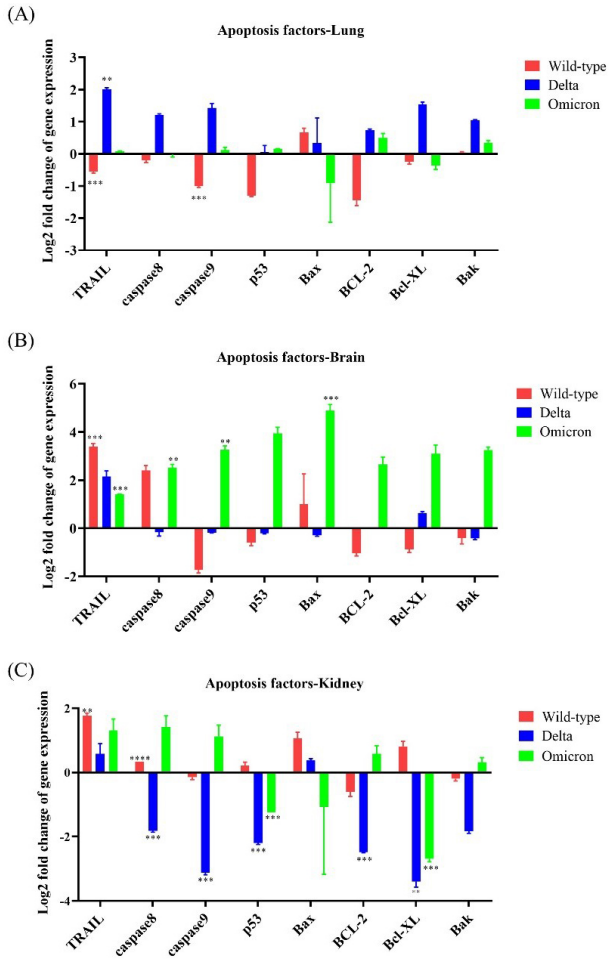

Fig. 6. Expression levels of apoptotic genes in K18-hACE2 mice infected with SARS-CoV-2 variants. The expression levels of eight apoptotic factor-related genes (*TRAIL*, *caspase 8*, *caspase 9*, *p53*, *Bax*, *BCL-2*, *Bcl-XL*, and *Bak*) were evaluated after infection with wild-type, Delta variant, or Omicron variant. (A) mRNA expression of apoptotic genes in the lungs after inoculation with wild-type, Delta, or Omicron. (B) mRNA expression of apoptotic genes in the brain after inoculation with wild-type, Delta, or Omicron. (C) mRNA expression of apoptotic genes in the kidney after inoculation with wild-type, Delta, or Omicron. * $p < 0.05$, ** $p < 0.01$, *** $p < 0.001$, **** $p < 0.0001$.

but significantly downregulated in the lungs (0.18-fold). Moreover, the lung and brain tissues of wild-type- and Delta-infected mice showed differential expression levels of *CCL21A*, *CXCL10*, and *CXCL12* (13.43-fold, 49.51-fold, and 0.04-fold, respectively). A more than 3-fold increase in expression was observed in the kidneys of mice infected with the Delta variant (Figs. 2A,B,5A–C).

3.3.4 Apoptotic Factor Expression

Apoptotic factors, including *caspase 8*, *caspase 9*, *p53*, *Bax*, *Bak*, *BCL-2*, and *Bcl-XL*, were mainly expressed in brain tissues of Omicron-infected mice; neither the lung nor the kidney showed more than 3-fold upregulation of these apoptotic factors. *TRAIL* was upregulated by >3-fold in the lung, brain, and kidney of Delta-infected mice and the brain of wild-type-infected mice. *Caspase 8* was upregulated in brain tissues after infection with the Delta or Omicron variants (Fig. 6B). In contrast to the brain of Omicron-infected mice, the kidneys of Delta-infected mice exhibited downregulated (<3-fold) expression levels of the apoptotic factors *caspase 8*, *caspase 9*, *p53*, *Bak*, *BCL-2*, and *Bcl-XL* (Fig. 6A–C).

3.4 Histopathology of the Lungs of SARS-CoV-2 Infected Mice

To compare the disease severity caused by the SARS-CoV-2 variants, the lung pathology of K18-hACE2 transgenic mice infected with the wild-type, Delta, and Omicron was observed at 6 d.p.i. after H&E staining. No signs of pneumonia were observed in the lung tissues of PBS mock mice (Fig. 7A). In contrast, mice infected with the wild-type showed signs of severe interstitial pneumonia, which is characterized by inflammatory cell infiltration (Fig. 7B). The lung tissue of mice infected with the Delta variant exhibited mild pneumonia (Fig. 7C). Interestingly, the lung tissues of mice infected with the Omicron variant exhibited considerably milder interstitial pneumonia than those of mice infected with the Delta variant (Fig. 7D).

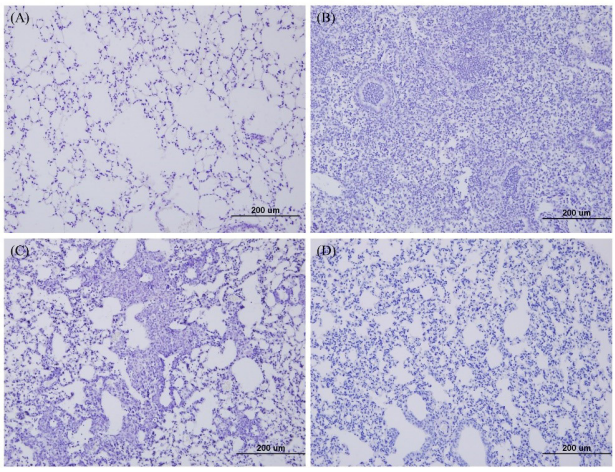

Fig. 7. Lung histopathology of K18-hACE2 transgenic mice infected with SARS-CoV-2 variants. At 6 d.p.i., the lung tissues of mice infected with the wild type, Delta, or Omicron variants were collected, and hematoxylin and eosin staining was performed. Lung histopathology was used to compare disease severity caused by each variant and wild-type. (A) Lung tissue of mock-infected mice. (B) Lung tissue of wild-type-infected mice. (C) Lung tissue of Delta-infected mice. (D) Lung tissues of Omicron-infected mice.

4. Discussion

Among the known VOCs, the Delta and Omicron variants have been identified as dominant variants at different time points during the COVID-19 pandemic and are still persistent in the human population. Although the Delta variant has been reported to have overt pathogenicity, Omicron is the most recent variant reported to have remarkably attenuated pathogenicity and robust transmissibility [21,22]. The pathogenicity of a viral pathogen depends on three factors: the accessibility of the virus to the host tissue, host cell susceptibility to virus multiplication, and virus susceptibility to host defense mechanisms [23].

Considering the outbreak indices, we focused on the pathogenicity profiles of the wild-type and the variants Delta and Omicron by analyzing the expression of immune response-related genes and the dynamics of infections in K18-hACE2 transgenic mice. Our results revealed that the wild-type and Delta variant resulted in a pronounced weight loss from 4 d.p.i. until death *in vivo*. In contrast, mice infected with the Omicron variant did not lose weight and survived until study termination. Moreover, our results indicated that the viral burden in the Omicron-infected K18-hACE2 mice was lower than that in the Delta- and wild-type-infected mice. Collectively, our results reveal that the Omicron variant exhibited lower pathogenicity in K18-hACE2 mice than the Delta variant and wild-type, which is consistent with the preliminary findings on the pathogenicity of SARS-CoV-2 in humans. Moreover, multiorgan tropism, including in the brain and kidney, was observed in the Delta- and Omicron-infected K18-hACE2 mice as well as in the infection of wild-type. The tissue tropism of the SARS-CoV-2 variants may be mainly attributed to the enhanced affinity and accessibility of the S protein to the ACE2 receptor. Although Omicron-infected mice showed lower viral loads in the lung, brain, and kidney tissues compared to those infected with the wild-type or Delta variant, the nasal turbinate of the Omicron-infected mice had significant viral titer even after 6 d.p.i. This may explain viral shedding and transmissibility associated with Omicron.

Other research works conducted using K18-hACE2 mice showed significantly attenuated replication of Omicron (B1.1.529) in lung and brain implying similar results to our findings [24–26]. As reported by Meng *et al.* [27] the impaired cleavage of spike protein and inefficient usage of TMPRSS2 cellular protein which is required in cell entry are the factors associated with the lower replication of Omicron compared to the other SARS-CoV-2 variants.

Most COVID-19 complications occur due to the dysregulated immune response caused by SARS-CoV-2 infection. Inflammation and cell death have been proposed as major mechanisms underlying severe COVID-19 [28–31]. Our findings indicate that the wild-type and the Delta variant result in a more pronounced upregulation of *TLR*, cytokine, and chemokine genes compared to the Omicron variant. Moreover, genes that were differentially expressed in wild-type- and Delta-infected mice overlapped closely, showing similar disease progression patterns. Although *TLR* and cytokine expression was lower in Omicron-infected mice, high apoptotic factors-related gene expression levels were observed in these mice, especially in the brain, suggesting immune evasion. These results suggest that the Omicron variant is more evolved than the other SARS-CoV-2 variants.

In SARS-CoV-2 infections, *TLR*s act as double-edged swords that induce immune-mediated pathology

rather than preventing the progression of infection [32–34]. Among *TLR*s, *TLR2* recognizes SARS-CoV-2 and other β-coronaviruses and may subsequently promote the secretion of inflammatory cytokines (*IL-6*, *IFN-*γ, *TNF*) and chemokines (*CXCL10*) and create dysregulated immune responses during SARS-CoV-2 infection [35,36]. Similarly, our results indicate that *TLR2* expression was substantially high in wild-type- and Delta-infected mice, accompanied by high mRNA transcription levels of *TNF-*α and *IFN-*γ. Moreover, another study has reported that severe SARS-CoV-2 pathogenicity was associated with upregulated expression levels of *TLR1*, *TLR4*, *TLR5*, *TLR8*, and *TLR9*, whereas moderate cases were associated with increased levels of *TLR7* [35]. Consistent with these results, our study revealed the upregulation of *TLR1*, *TLR2*, *TLR7*, *TLR8*, and *TLR9* following SARS-CoV-2 infection.

Cytokines are key drivers of inflammatory responses, which directly modulate disease severity [37]. Many studies have described the increased expression of cytokines, including *IL-1/2/4/6/10/17*, *IFN-I/II/III*, *TNF*, *G-CSF*, *GM-CSF*, *MCP-1*, *MIP-1*α, and *IP-10* in patients with COVID-19 [38–40]. *IL-17* promotes the production of other proinflammatory mediators (*IL-1*, *IL-6*, *TNF-*α) but does not affect host antiviral gene expression upon infection with respiratory viruses [41]. *IL-17A* is considered the silent amplifier of COVID-19 as it stimulates neutrophils in patients with severe COVID-19 [39,42], increases the viral load, and worsens disease severity [43]. Interestingly, in our study, we observed increased *IL-17A* levels mainly in the lung of wild-type- and Delta-infected mice, confirming the higher pathogenicity of the wild-type and Delta SARS-CoV-2 viruses. Another study reported that elevated *G-CSF* and *GM-CSF* levels have been observed in patients with COVID-19 who required ICU admission [39]. Moreover, we also observed *IL-1*-stimulated *G-CSF* and *GM-CSF* production by Th17 cells in the lungs of wild-type-infected mice and brains of Delta-infected mice, respectively. These factors play a vital role in inflammatory processes by stimulating the proliferation and activation of macrophages, eosinophils, and neutrophils. Another important cytokine: *IL-10* has been reported with dramatic expression in COVID-19 patients as initial response to the virus and it has correlated with the expression of elevated *IL-6* [44]. Moreover, *IL-12*, *IL-27* and *IL-21* have reported to affect the upregulation of *IL-10* expression by T helper 1 cells [45–47] and *IL-4* also mediates in increase expression of *IL-10* in Lipopolysaccharide (LPS) stimulated macrophages [48]. Enhanced levels of *IL-4* and *IL-6* in our study implicate the elevation of *IL-10* in COVID-19 patients.

In addition to cytokines, we also observed overexpression of chemokines in our study. Chemokine-mediated acute respiratory complications have been reported to be associated with 40% of deaths. Furthermore, we observed increased expression levels of *TLR*s, cytokines, and chemokines in the kidney, especially in Delta-infected mice, which may lead to acute kidney injury (AKI) as a complication of long-term COVID-19 infections. Our results are consistent with several studies reporting that patients with COVID-19 infected with the Delta variant experienced lingering AKI [49,50].

Moreover, programmed cell death has been proposed as a pathway for SARS-CoV-2 pathogenesis [51]. In agreement with this hypothesis, in our study, Omicron-infected mice expressed higher levels of apoptotic factors compared to mice infected with the other two SARS-CoV-2 variants. Elevated expression levels of caspase 8 and caspase 9 in the brain tissues of the Omicron infected mice ratified the involvement of caspase mediated apoptotic pathways in SARS-CoV-2 infection. The experiments using Vero E6 cells have reported that the activation of *caspase 8* and *9* and *BID* was induced by the SARS-CoV-2 ORF3a which ultimately results the cell death [52]. Upregulation of *Bax*, and *BAK* genes which cause the mitochondrial outer membrane permeabilization provide evidence for the activation of intrinsic pathway of apoptosis cell death by Omicron in the brain. However, the opening of the gateways of caspase 8 ultimately initiates apoptosis [53].

Our study stressed that even though the impaired Omicron viral replication in the brain, it can cause the upregulation of certain apoptosis factor related genes. This result complies with the findings of Frank *et al*. [54]; the S1 subunit of spike protein of SARS-CoV-2 is solely enough to act as a pathogen associated molecular pattern (PAMP) and drive the neuroinflammatory responses independent of viral infection. However, the low viral titers in brain shown with Omicron was not found to be associated with either the neuropathological changes or levels of immune response gene expression [55,56]. Similarly, RT-qPCR and immunohistopathological analysis of brain tissues of de positive patients by Matschke *et al*. [57] has confirmed the presence of SARS-CoV-2 virus in brain even though it's not correlated with the neuropathology of brain. Our results also corroborated with the above-mentioned research findings on differences of viral titer and the neuropathological changes.

As Omicron induce the programmed cell death associated immune responses in brain, the central nervous system associated manifestations might be occurred in the Long COVID sequelae. The experiment in mice provides evidence for persistent post-acute neurological complications after exposure to COVID-19 [58]. Another study which uses cohort of COVID-19 patients has reported the participants diagnosed with the neurological conditions including memory impairment, cerebrovascular disorders, cognition and sensory disorders in post-acute phase and furthermore COVID-19 patients have a 42% risk of developing neurological complications within a year post infection [59,60]. Not only neurological complications but also pulmonary, cardiovascular, endocrine, hematologic, renal, gastrointestinal, dermatologic, immunological issues

were encompassed by long COVID sequelae [60]. Therefore, therapeutic and diagnostic algorithms should be aided for the resolution of consequences of acute and post-acute COVID conditions.

In addition, our histopathology results suggest that severe pneumonia in the lungs of wild-type- and Delta-infected mice may have arisen due to a cytokine storm resulting from the increased levels of cytokines and chemokines.

5. Conclusions

Our study revealed that the pathogenicity of SARS-CoV-2 varies in the following order: wild-type >Delta variant >Omicron variant. Wild-type SARS-CoV-2 exhibited the highest pathogenicity, which is mediated by inflammatory cytokines that contribute to cytokine storms. The pathogenicity of the Delta variant is also driven by increased cytokine and chemokine expression levels. Omicron infection results in upregulated programmed cell death pathways, indicating invasion of host antiviral defenses by the Omicron variant. In conclusion, our study provides insights into host immune responses to several SARS-CoV-2 variants, which may help in the development of therapeutic strategies against SARS-CoV-2.

Availability of Data and Materials

The data are available from the corresponding author upon reasonable request.

Author Contributions

SHS designed the research study. All authors performed the research. SHS provided help and advice on experiments. KAPPK and YJ analyzed the data and wrote the manuscript. All authors contributed to editorial changes in the manuscript. All authors read and approved the final manuscript.

Ethics Approval and Consent to Participate

All experiments involving animals were approved by the Internal Animal Use Committee at Chungnam National University (CNU) (Approval: 202206A-CNU-124). The research work was performed according to the guidelines and regulations of CNU, the Republic of Korea.

Acknowledgment

We would like to thank Editage (https://www.editage.com) for English language editing.

Funding

This work was partly supported by a grant by the National Research Foundation of Korea (NRF) funded by the Korean government (MSIT) (2019R1A2C2002166812).

Conflict of Interest

The authors declare no conflict of interest. Sang Heui Seo was serving as Guest Editor of this journal. We declare that Sang Heui Seo had no involvement in the peer review of this article and has no access to information regarding its peer review. Full responsibility for the editorial process for this article was delegated to Vijay Kumar.

Supplementary Material

Supplementary material associated with this article can be found, in the online version, at https://doi.org/10.31083/j.fbl2711316.

References

[1] Hasoksuz M, Kilic S, Sarac F. Coronaviruses and SARS-COV-2. Turkish Journal of Medical Sciences. 2020; 50: 549–556.

[2] Allen H, Tessier E, Turner C, Anderson C, Blomquist P, Simons D, *et al*. Comparative Transmission of SARS-CoV-2 Omicron (B.1.1.529) and Delta (B.1.617.2) Variants and the Impact of Vaccination: National Cohort Study. England. 2022. (preprint)

[3] Liu Z, Xiao X, Wei X, Li J, Yang J, Tan H, *et al*. Composition and divergence of coronavirus spike proteins and host ACE2 receptors predict potential intermediate hosts of SARS-CoV-2. Journal of Medical Virology. 2020; 92: 595–601.

[4] Lvov DK, Alkhovsky SV. Source of COVID-19 Pandemic: Ecology and Genetics of Coronaviruses (Betacoronavirus: Coronaviridae) SARS-CoV, SARS-CoV-2 (Subgenus Sarbecovirus), and MERS-CoV (Subgenus Merbecovirus). Problems of Virology. 2020; 65: 62–70.

[5] World Health Organization. Tracking SARS-CoV-2 Variants. 2022. Available at: https://www.who.int/en/activities/tracking-SARS-CoV-2-variants/ (Accessed: 31 May 2022).

[6] Kumar S, Thambiraja TS, Karuppanan K, Subramaniam G. Omicron and Delta variant of SARS-CoV-2: a comparative computational study of spike protein. Journal of Medical Virology. 2022; 94: 1641–1649.

[7] Zhan Y, Yin H, Yin JY. B.1.617.2 (Delta) Variant of SARS-CoV-2: features, transmission and potential strategies. International Journal of Biological Sciences. 2022; 18: 1844–1851.

[8] World Health Organization. Classification of Omicron (B.1.1.529): SARS-CoV-2 Variant of Concern. 2021. Available at: https://www.who.int/news/item/26-11-2021-classification-of-omicron-(b.1.1.529)-sars-cov-2-variant-of-concern (Accessed: 31 May 2022).

[9] Sigal A, Milo R, Jassat W. Estimating disease severity of Omicron and Delta SARS-CoV-2 infections. Nature Reviews Immunology. 2022; 22: 267–269.

[10] Hsu RJ, Yu WC, Peng GR, Ye CH, Hu S, Chong PCT, *et al*. The Role of Cytokines and Chemokines in Severe Acute Respiratory Syndrome Coronavirus 2 Infections. Frontiers in Immunology. 2022; 13: 832394.

[11] Jafarzadeh A, Chauhan P, Saha B, Jafarzadeh S, Nemati M. Contribution of Monocytes and Macrophages to the Local Tissue Inflammation and Cytokine Storm in COVID-19: Lessons from SARS and MERS, and Potential Therapeutic Interventions. Life Sciences. 2020; 257: 118102.

[12] Bao L, Deng W, Huang B, Gao H, Liu J, Ren L, *et al*. The Pathogenicity of SARS-CoV-2 in hACE2 Transgenic Mice. Nature. 2020; 583: 830–833.

[13] Dong W, Mead H, Tian L, Park J, Garcia JI, Jaramillo S, *et al*. The K18-Human ACE2 Transgenic Mouse Model Recapitulates Non-severe and Severe COVID-19 in Response to an Infectious

Dose of the SARS-CoV-2 Virus. Journal of Virology. 2022; 96: e0096421.
[14] Natekar JP, Pathak H, Stone S, Kumari P, Sharma S, Auroni TT, *et al*. Differential Pathogenesis of SARS-CoV-2 Variants of Concern in Human ACE2-Expressing Mice. Viruses. 2022; 14: 1139.
[15] Winkler ES, Bailey AL, Kafai NM, Nair S, McCune BT, Yu J, *et al*. SARS-CoV-2 infection in the lungs of human ACE2 transgenic mice causes severe inflammation, immune cell infiltration, and compromised respiratory function. BioRxiv. 2020. (preprint).
[16] Takao K, Miyakawa T. Genomic responses in mouse models greatly mimic human inflammatory diseases. Proceedings of the National Academy of Sciences. 2015; 112: 1167–1172.
[17] Jiang R, Liu M, Chen Y, Shan C, Zhou Y, Shen X, *et al*. Pathogenesis of SARS-CoV-2 in Transgenic Mice Expressing Human Angiotensin-Converting Enzyme 2. Cell. 2020; 182: 50–58.
[18] Park JG, Pino PA, Akhter A, Alvarez X, Torrelles JB, Martinez-Sobrido L. Animal Models of COVID-19: Transgenic Mouse Model. SARS-CoV-2 (pp. 259–289). Humana: New York, NY, 2022.
[19] Winkler ES, Bailey AL, Kafai NM, Nair S, McCune BT, Yu J, *et al*. Publisher Correction: SARS-CoV-2 infection of human ACE2-transgenic mice causes severe lung inflammation and impaired function. Nature Immunology. 2020; 21: 1470–1470.
[20] Reed LJ and Muench H. A Simple Method of Estimating fifty Percent Endpoints. American Journal of Hygiene. 1938; 27: 493–497.
[21] Chu H, Yuen K. Pathogenicity of SARS-CoV-2 Omicron. Clinical and Translational Medicine. 2022; 12: e880.
[22] Veneti L, Bøås H, Bråthen KA, Stålcrantz J, Bragstad K, Hungnes O, *et al*. Reduced Risk of Hospitalisation among Reported COVID-19 Cases Infected with the SARS-CoV-2 Omicron BA.1 Variant Compared with the Delta Variant, Norway, December 2021 to January 2022. Eurosurveillance Journal. 2022; 27: 2200077.
[23] Samuel Baron MF, Thomas A. Viral Pathogenesis in Medical Microbiology, Galveston (TX): University of Texas Medical Branch at Galveston, 1996.
[24] Natekar JP, Pathak H, Stone S, Kumari P, Sharma S, Auroni TT, *et al*. Differential pathogenesis of SARS-CoV-2 variants of concern in human ACE2-expressing mice. Viruses. 2022; 14: 1139.
[25] Halfmann PJ, Iida S, Iwatsuki-Horimoto K, Maemura T, Kiso M, Scheaffer SM, *et al*. SARS-CoV-2 Omicron virus causes attenuated disease in mice and hamsters. Nature. 2022; 603: 706–714.
[26] Shuai H, Chan JF, Hu B, Chai Y, Yuen TT, Yin F, *et al*. Attenuated replication and pathogenicity of SARS-CoV-2 B.1.1.529 Omicron. Nature. 2022; 603: 693–699.
[27] Meng B, Abdullahi A, Ferreira IATM, Goonawardane N, Saito A, Kimura I, *et al*. Altered TMPRSS2 usage by SARS-CoV-2 Omicron impacts infectivity and fusogenicity. Nature. 2022; 603: 706–714.
[28] Kang YW, Park S, Lee KJ, Moon D, Kim YM, Lee SW. Understanding the Host Innate Immune Responses against SARS-CoV-2 Infection and COVID-19 Pathogenesis. Immune Network. 2021; 21.
[29] Lee S, Channappanavar R, Kanneganti T. Coronaviruses: Innate Immunity, Inflammasome Activation, Inflammatory Cell Death, and Cytokines. Trends in Immunology. 2020; 41: 1083–1099.
[30] Li X, Zhang Z, Wang Z, Gutiérrez-Castrellón P, Shi H. Cell deaths: Involvement in the pathogenesis and intervention therapy of COVID-19. Signal Transduction and Targeted Therapy. 2022; 7: 186.
[31] Ren Y, Wang A, Fang Y, Shu T, Wu D, Wang C, *et al*. SARS-CoV-2 Membrane Glycoprotein M Triggers Apoptosis with the Assistance of Nucleocapsid Protein N in Cells. Frontiers in Cellular and Infection Microbiology. 2021; 627.
[32] Huang B, Zhao J, Unkeless JC, Feng ZH, Xiong H. TLR Signaling by Tumor and Immune Cells: a Double-Edged Sword. Oncogene. 2008; 27: 218–224.
[33] Kayesh MEH, Kohara M, Tsukiyama KK. An Overview of Recent Insights into the Response of TLR to SARS-CoV-2 Infection and the Potential of TLR Agonists as SARS-CoV-2 Vaccine Adjuvants. Viruses. 2021; 13: 2302.
[34] Yokota S, Okabayashi T, Fujii N. The Battle between Virus and Host: Modulation of Toll-Like Receptor Signaling Pathways by Virus Infection. Mediators of Inflammation. 2010; 2010: 1–12.
[35] Sariol A, Perlman S. SARS-CoV-2 takes its Toll. Nature Immunology. 2021; 22: 801–802.
[36] Zheng M, Karki R, Williams EP, Yang D, Fitzpatrick E, Vogel P, *et al*. TLR2 Senses the SARS-CoV-2 Envelope Protein to produce inflammatory cytokines. Nature Immunology. 2021; 22: 829–838.
[37] Borish LC, Steinke JW. 2. Cytokines and Chemokines. Journal of Allergy and Clinical Immunology. 2003; 111: S460–S475.
[38] Chen C, Zhang X, Ju ZY, He WF. Advances in the Research of Mechanism and Related Immunotherapy on the Cytokine Storm Induced by Coronavirus Disease 2019. Chinese Journal of Burns. 2020. 36: 471–475.
[39] Huang C, Wang Y, Li X, Ren L, Zhao J, Hu Y, *et al*. Clinical Features of Patients Infected with 2019 Novel Coronavirus in Wuhan, China. The Lancet. 2020; 395: 497–506.
[40] Wang W, Liu X, Wu S, Chen S, Li Y, Nong L, *et al*. The definition and risks of Cytokine Release Syndrome-Like in 11 COVID-19-Infected Pneumonia critically ill patients: Disease Characteristics and Retrospective Analysis. The Journal of Infectious Diseases. 2020; 222: 1444–1451.
[41] Ryzhakov G, Lai CC, Blazek K, To K, Hussell T, Udalova I. IL-17 Boosts Proinflammatory Outcome of Antiviral Response in Human Cells. The Journal of Immunology. 2011; 187: 5357–5362.
[42] Xu Z, Shi L, Wang Y, Zhang J, Huang L, Zhang C, *et al*. Pathological findings of COVID-19 associated with acute respiratory distress syndrome. The Lancet Respiratory Medicine. 2020; 8: 420–422.
[43] Liu Y, Zhang C, Huang F, Yang Y, Wang F, Yuan J, *et al*. 2019-novel coronavirus (2019-nCoV) infections trigger an exaggerated cytokine response aggravating lung injury. 2020. Available at: http://www.chinaxiv.org/abs/202002.00018 (Accessed: 12 February 2020).
[44] Jin J, Han X, Yu Q. Interleukin-6 induces the generation of IL-10-producing Tr1 cells and suppresses autoimmune tissue inflammation. Journal of Autoimmunity. 2013; 40: 28–44.
[45] Saraiva M, Christensen JR, Veldhoen M, Murphy TL, Murphy KM, O'Garra A. Interleukin-10 Production by Th1 Cells Requires Interleukin-12-Induced STAT4 Transcription Factor and ERK MAP Kinase Activation by High Antigen Dose. Immunity. 2009; 31: 209–219.
[46] Fitzgerald DC, Zhang G, El-Behi M, Fonseca-Kelly Z, Li H, Yu S, *et al*. Suppression of autoimmune inflammation of the central nervous system by interleukin 10 secreted by interleukin 27–stimulated T cells. Nature Immunology. 2007; 8: 1372–1379.
[47] Spolski R, Kim H, Zhu W, Levy DE, Leonard WJ. IL-21 Mediates Suppressive Effects via its Induction of IL-10. The Journal of Immunology. 2009; 182: 2859–2867.
[48] Cao S, Liu J, Song L, Ma X. The Protooncogene c-Maf is an Essential Transcription Factor for IL-10 Gene Expression in Macrophages. The Journal of Immunology. 2005; 174: 3484–3492.
[49] McAdams M, Ostrosky-Frid M, Rajora N, Hedayati S. Effect of COVID-19 on Kidney Disease Incidence and Management.

Kidney360. 2021; 2: 141.
[50] McAdams MC, Xu P, Saleh SN, Li M, Ostrosky-Frid M, Gregg LP, *et al*. Risk Prediction for Acute Kidney Injury in Patients Hospitalized with COVID-19. Kidney Medicine. 2022; 4: 100463.
[51] Morais da Silva M, Lira de Lucena AS, Paiva Júnior SDSL, Florêncio De Carvalho VM, Santana de Oliveira PS, da Rosa MM, *et al*. Cell Death Mechanisms Involved in Cell Injury Caused by SARS-CoV-2. Reviews in Medical Virology. 2022; 32: e2292.
[52] Ren Y, Shu T, Wu D, Mu J, Wang C, Huang M, *et al*. The ORF3a protein of SARS-CoV-2 induces apoptosis in cells. Cellular and Molecular Immunology. 2020; 17: 881–883.
[53] Bader SM, Cooney JP, Pellegrini M, Doerflinger M. Programmed Cell Death: the Pathways to Severe COVID-19? The Biochemical Journal. 2022; 479: 609–628.
[54] Frank MG, Nguyen KH, Ball JB, Hopkins S, Kelley T, Baratta MV, *et al*. SARS-CoV-2 spike S1 subunit induces neuroinflammatory, microglial and behavioral sickness responses: Evidence of PAMP-like properties. Brain, Behavior, and Immunity. 2022; 100: 267–277.
[55] Solomon IH, Normandin E, Bhattacharyya S, Mukerji SS, Keller K, Ali AS, *et al*. Neuropathological Features of Covid-19. New England Journal of Medicine. 2020; 383: 989–992.
[56] Thakur KT, Miller EH, Glendinning MD, Al-Dalahmah O, Banu MA, Boehme AK, *et al*. COVID-19 Neuropathology at Columbia University Irving Medical Center/New York Presbyterian Hospital. Brain. 2021; 144: 2696–2708.
[57] Matschke J, Lütgehetmann M, Hagel C, Sperhake JP, Schröder AS, Edler C, *et al*. Neuropathology of patients with COVID-19 in Germany: a post-mortem case series. The Lancet Neurology. 2020; 19: 919–929.
[58] Fernández-Castañeda A, Lu P, Geraghty AC, Song E, Lee MH, Wood J, *et al*. Mild respiratory COVID can cause multi-lineage neural cell and myelin dysregulation. Cell. 2022; 185: 2452–2468.
[59] Al-Aly Z, Bowe B, Xie Y. Long COVID after breakthrough SARS-CoV-2 infection. Nature Medicine. 2022; 28: 1461–1467.
[60] Stefanou MI, Palaiodimou L, Bakola E, Smyrnis N, Papadopoulou M, Paraskevas GP, *et al*. Neurological manifestations of long-COVID syndrome: A narrative review. Therapeutic Advances in Chronic Disease. 2022; 13: 20406223221076890.